Journal of Applied Polymer Science

Rapid Fabrication of Organic/Organic Photonic Bandgap Films with Tuneable Mechanical Properties Using Blended Polymer Spheres

Yu-Cheng Kuo,[1] Meng-Chu Chen,[2] Tsung-Te Lin,[3] Yi-Ru Shiu,[3] Hui Chen[1]

[1]Department of Chemical and Materials Engineering, National Central University, Jhongli, Taiwan, Republic of China
[2]Department of Applied Science, National Taitung University, Taitung, Taiwan, Republic of China
[3]Institute of Nuclear Energy Research, Atomic Energy Council, Taoyuan, Taiwan, Republic of China
Correspondence to: H. Chen (huichen@cc.ncu.edu.tw)

ABSTRACT: In this study, the photonic bandgap (PBG) film with tunable mechanical properties and photonic stop band was prepared by a simple and feasible approach. Colloid polymer spheres with a relatively large diameter (approximate D_n of 200 nm) and different glass transition temperatures (T_g) were blended with small polystyrene (PS) latex ($D_n = 20$ nm) and were subsequently casted on a substrate for 3 h at 50°C for self-assembly of the PBG film. The monodispersed polymer spheres were synthesized by soap-free emulsion polymerization in the boiling state. The T_g values of the spheres were predetermined based on the Fox equation, and designed to fall in the region of −34°C to 112°C. Small PS could also be synthesized by this approach using the comonomer, sodium *p*-styrenesulfonate (NaSS), to ensure the small diameter. The long-range ordered structure constructed by embedding the small PS in the PBG film was indirectly confirmed on the basis of SEM analysis, from which the monochromatic film color was determined based on Bragg's diffraction law. Tunable film color was achieved by adjusting the diameter of the spheres, as evaluated using UV–Vis. Tunable mechanical properties of the PBG film were also achieved by varying the T_g of the spheres or the filling ratio of small PS. Based on these approaches, the ultimate tensile strength could be tuned in the region between 0.39 to 4.7 Mpa, and the relative strain could be varied from 1236% to 16%, illustrative of the excellent deformability of the film. Furthermore, by variation of these two parameters, the film properties could be changed from typical elastomer behavior to brittle plastic polymer type behavior, greatly extending the prospective application fields. © 2013 Wiley Periodicals, Inc. J. Appl. Polym. Sci. **2014**, *131*, 40276.

KEYWORDS: colloids; applications; films; optical properties

Received 26 August 2013; accepted 8 December 2013
DOI: 10.1002/app.40276

INTRODUCTION

In recent decades, photonic crystals (PCs) or photonic bandgap (PBG) materials have emerged as promising materials due to their unique light attenuation properties. The specific periodic dielectric (or refractive index) architectural construction of these species can strongly confine and control the propagation of electromagnetic (EM) waves for certain frequency ranges,[1–4] thereby giving rise to the PBG. Thus, extensive and prospective development of many applications such as smart windows, chemical sensors, optical devices, and memory devices[5–11] is based on these features.

The numerous approaches for construction of PBG materials can be roughly classified into two categories, i.e., top–down and bottom-up methods.[12] The top–down approaches are often carried out using traditional microfabrication techniques, such as photolithography and etching,[13–16] to produce periodical structures with the desired shape from bulk materials. The bottom–up approach generally exploits the self-assembly of the molecular species or colloid spheres into one-, two-, and three-dimensional periodic structures.[17,18] The assembly of colloidal spheres is the most commonly employed strategy for constructing PBG materials given its relatively simple procedure and cost-efficiency for large-scale production.[19,20] Typical colloidal crystals are ordered arrays of highly monodisperse oxides or polymer spheres because these species can readily be synthesized with the desired diameter.[21] The sol–gel process is typically employed for synthesis of oxide materials such as SiO_2, TiO_2, and ZnO, whereas the conventional polymer spheres of PS, PMMA, and their cross-linked products are generally synthesized by soap-free emulsion polymerization (or using surfactants).[21–24] However, such colloid spheres are always "hard" beads. Consequently, the photonic crystal films constructed using these spheres exhibit less than satisfactory mechanical properties.

To resolve these issues, a number of interesting approaches for the construction of PBG films with high toughness have been

developed.[25–31] These strategies can be classified into two divisions. The first approach achieves enhanced linkage among the colloid spheres by various means, such as sintering the PBG film at high temperature,[32,33] or coating the polymer PBG with a thin silica layer.[34] However, a more effective method involves direct arrangement of narrow-size modified, or core–shell spheres into the PBG film. For example, Leyrer's group synthesized various modified spheres with different functional groups on the surface of the spheres and subsequently assembled them to generate covalent or physical cross-linking among the PBG films. In this way, a 10-fold enhancement of the chemomechanical stability of the PBG films was achieved.[30] Successful construction of tough PBG films has also been reported using rigid core/soft shell spheres such as polystyrene (PS)/poly(butylmethacrylate), PS/poly(methyl methacrylate-acrylic acid), and PS/poly(*N*-isopropylacrylamide)[19,25,35] by arrangement of the rigid cores into periodical lattices, while the soft shell provides the binding force between the surfaces of the spheres. In the second approach, instead of simply enhancing the binding force between the contact areas of the spheres only, prepolymers or monomers are introduced into the voids of the colloidal crystal, which are subsequently cured or polymerized to directly replace the air void with the elastic polymer, thus increasing the binding area. For example, Fudouzi's group fabricated an elastic silicone PBG film with reversibly tunable color by embedding the ordered PS colloid into poly(dimethylsiloxane) (PDMS).[36] Fougler's group demonstrated that a similar film could also be fabricated by locking the PS colloid crystal in water-free polyacrylate, with a consequent shift of the bandgap by more than 300 nm.[37–39] A particularly unique technique was published by Hellmann and co-workers, demonstrating that tough PBG films devoid of air voids could be obtained based on the use of a cross-linked PS core and soft polyacrylate shell spheres which assist the melt-flow process.[40–50] Although these strategies can be successfully used to prepare tough PBG films, the synthesis of core–shell spheres is necessarily tedious and multi-step film-formation processes are required.

Thus, since 2009, Wu and co-workers published a series of literature[29,51–53] describing an attractive, novel, and simple approach for constructing tough PBG films. This approach is different from the use of normal colloid PBG films using hard spheres as periodical lattices, in that the tough films were constructed based on soft monodispersed spheres by binding with nanosilica particles. In this manner, the binding force was directly supplied by the entirety of the soft spheres, thus, the film exhibited sufficient mechanical durability to withstand further processing, e.g., cutting, puckering, bending etc.[53] Although the film-formation processes were relatively simple, the PBG films still had to be self-assembled from blended suspensions at room temperature over the course of one day. Furthermore, the contrast in the refractive index was mainly between the organic polymer and inorganic SiO_2, where the synthesis of inorganic silica particles is necessarily time-consuming and these species are not readily complexed, and their physical properties are not easily changed by surface modification. To simplify the preparation procedures and extend the application fields, the SiO_2 nanoparticles with high refractive index were replaced with a designed organic nanoparticle to construct an organic/organic matrix, without inclusion of any inorganic portion in the PBG films. Based on our previous work,[19,54,55] monodispersed polymer spheres with the desired T_g, diameter, and even core–shell structure were easily synthesized within 2 h in the boiling state. In this study, we evaluate the changes in the interaction between the two categories of spheres with variation of the functional groups. Based on this concept, soft monodispersed spheres with various T_g are readily synthesized using small PS and are subsequently blended with each other for self-assembly at 50°C over 3 h to generate the PBG films. The entire duration of the reaction, from the synthesis of the spheres to complete assembly, is only 5 h. Variation of the PGB is achieved by changing the diameter of the soft spheres, and the mechanical properties of the PBG film are easily tailored from typical elastomer behavior to brittle plastic polymer type behavior by tuning the sphere T_g or filling ratio of small PS.

EXPERIMENTAL

Materials

The reagent-grade monomers, styrene (St), methacrylic acid (MAA), and sodium *p*-styrenesulfonate (NaSS) were purchased from SHOWA. Butyl methacrylate (BMA) and butyl acrylate (BA) were obtained from Acros. All monomers were purified by vacuum distillation. Potassium persulfate (KPS), used as the initiator, was acquired from SHOWA.

Preparation of Spheres with Different T_g

Based on the Fox equation, monodisperse spheres with different T_g were designed by varying the feeding ratio of St, BMA, and BA. The formulations are shown in Table I. Initially, deionized water was mixed with the mixture of monomer and 540 μL MAA in a 250 mL three-necked flask equipped with a reflux condenser. The reaction mixture was mechanically stirred at 420 rpm, and the reaction temperature was then increased to achieve the boiling state. After 5 min, 5 g of deionized water, in which 0.0876 g of KPS was dissolved, was added to the reaction mixture. The polymerization reaction was terminated after 2 h. The particle diameter was estimated from SEM observation of more than 100 particles to ensure accuracy based on following equation:

$$D_n = \left(\sum n_i D_i / \sum n_i \right)$$

where the terms D_n, D_i, and n_i represent the number-averaged diameter, the particle diameter, and amount of particles, respectively.

Preparation of Small PS Spheres

Small PS spheres were synthesized by soap-free emulsion polymerization in the boiling state. The typical procedure is as follows: 85 g of deionized water, 10 g St, 0.6 g NaSS, and 540 μL of MAA were combined in a 250 mL three-necked flask. The reaction mixture was mechanically stirred at 420 rpm, and the reaction temperature was increased to achieve the boiling state. After 5 min, 5 g of deionized water containing 0.0876 g of dissolved KPS was added to the reaction mixture. The polymerization was stopped after 2 h.

Fabrication of Opal Films

Various sphere-suspensions with equal solid content (10 wt %) were blended with the required amount of small PS colloid, and magnetically stirred for 5 min. This dispersion was

Table I. The Preparation Conditions[a] and the Results from DLS and DSC of Polymer Spheres

St (g)	BMA (g)	BA (g)	$T_{g,\ Fox}$[b] (°C)	$T_{g,\ DSC}$[c] (°C)	N-mean[d] (d nm)	PdI[d]	D_n[e] (nm)
10	-	-	116	112	178	0.048	179
1.9	5.1	-	53	50	167	0.026	153
-	7	-	35	26	153	0.073	145
-	5.2	1.8	10	8	176	0.076	160
-	3.1	3.9	−15	−20	205	0.068	145
-	-	7	−45	−34	281	0.008	224

[a] Reaction condition : Total amount : 100 g, MAA, 5 wt %; KPS, 3.6 mM; reaction temperature, 100°C; reaction time, 2 h.
[b] Predicted by Fox equation.
[c] Determined from DSC.
[d] Determined from DLS.
[e] Number-averaged diameter was determined by a survey of 100 particles from SEM.

ultrasonically treated for 2 min, and 5 mL of suspended particles was subsequently spread onto a 10 × 10 cm polytetrafluoroethylene plate and dried at 50°C for 3 h. The water of latex was evaporated, during which the spheres in the latex were self-assembled into the ordered lattice.

RESULTS AND DISCUSSION

Fabrication and Structure of PBG Film

In this study, a series of PBG films were fabricated by casting the blended polymer suspension on the polytetrafluoroethylene substrate at 50°C for 3 h. The blended polymer suspension consisted of two categories of spheres distinguished by the sphere diameter. The latex of the copolymer spheres with larger diameter (approximate D_n of 200 nm) and various T_g, which were denoted polymer spheres for convenience, was then blended with the small PS ($D_n = 20$ nm) to produce the blended polymer suspension. These small PS can hamper deformation and coalescence between the soft spheres during the film-forming process. Thus, the monodisperse soft spheres can stack tightly after self-assembly, and the voids between the polymer spheres are filled with small PS to form a three-dimensional polymer–polymer ordered structure.

Correlated literature[52] indicated that the mechanical properties of the colloid PBG film were significantly affected by the T_g of the component particles. However, most of the reported colloid PBG films were constructed with core–shell spheres, or single category spheres, and only a few studies by Wu's group discussed blend PBG films.[29,51–53] Thus, to investigate the relationship between the sphere T_g and film properties, polymer spheres with different T_g were synthesized herein, the formulations and correlated analysis data of which are shown in Table I. The softness of the polymer spheres is dependent on the monomer feed-in proportion of St, BMA, and BA. A series of spheres with different T_g were designed based on the Fox equation, such that the predicted T_g values were in the region of −45°C to 116°C, which roughly corresponded to the measured values from DSC. The diameters of the spheres prepared from the mixture of the monomer of BMA and BA decreased as the proportion of BMA in the monomer mixture increased. This trend was attributed to the difference in the extent of water solubility of BMA (3 g/L) and BA (1.4 g/L). The higher water solubility of BMA furnishes more nuclei sites in the aqueous phase, while the polymerization process occurs during the particle nucleation stage. Thus, increasing the proportion of BMA in the monomer mixture produced a larger number of spheres, leading to the decrease in diameter. Similar results were also observed when St and BMA were used as the feed-in monomer. The diameter of the PS spheres was 178 nm, which was larger than that of the P(St-co-BMA) spheres of 167 nm. Comparison of the water solubility of St versus BMA showed that St (300 mg/L) was more difficult to dissolve in water, thus forming fewer nuclei sites at the particle nucleation stage, with consequent formation of fewer spheres with larger diameters. DLS results indicated that the spheres of each copolymer displayed low PDI (<0.08) values, which demonstrates that monodispersed copolymer spheres could be synthesized as the feed-in composition of the monomers was varied.

The small PS sample was synthesized with the aid of the NaSS comonomer to reduce the diameter. The PDI value of 0.139 derived from DLS indicated that the spheres exhibited mid-range polydispersity. However, the optical properties of the PBG

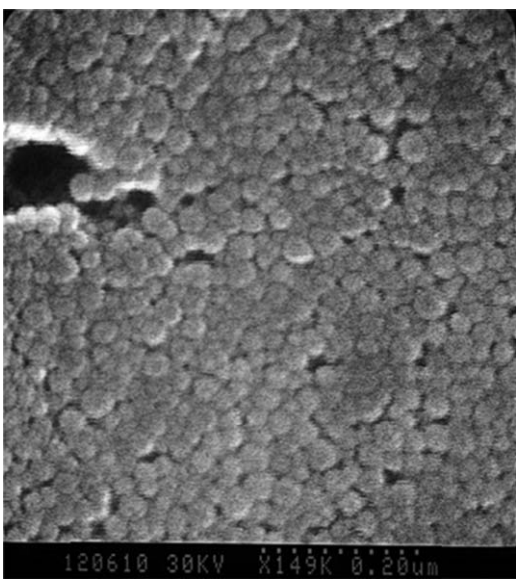

Figure 1. Surface morphologies of small PS spheres.

film were mainly determined by the periodical structure constructed by the polymer spheres. The small PS functioned only as the filler within the interstices of the PBG film. Thus, the diameter is the paramount parameter for ensuring that the internal structure is maintained, whereas the size should be smaller than the void between the polymer spheres. Based on the DLS analysis, the PS diameter (20 nm) was sufficiently small for use as a filler, and the surface morphologies are shown in Figure 1. The small PS sample exhibited a spherical morphology, and the diameter derived from SEM was analysis was consistent with the DLS result, i.e., distributed around 20 nm. The higher T_g and smaller diameter of the PS sample makes it useful as part of the framework of the PBG film after film formation.

The architectural arrangement of the PBG films prepared from polymer spheres with various T_g having a small PS content of 25 wt % was observed using SEM, and the upper surface and cross-sectional images are shown in Figure 2. Highly ordered, close-packed lattices with perfect face-centered cubic (FCC) array were observed for each of the samples. The polymer spheres were hexagonally arranged with the small PS occupying the interstices. These observations demonstrate that the polymer spheres of various T_g can self-assemble into three-dimensional periodic structures with the aid of the small PS colloid. The SEM images also revealed that the surface morphologies of the PBG films were significantly altered with variation of the T_g of the polymer spheres. In the case of the PBG film constructed using polymer spheres with a T_g of 112°C [Figure 2(a)], clear barrier ribs were observed between the interfaces of the polymer spheres, delineating the spherical shape with curved surface, and the distinct interior boundaries also indicated that the ribs were constructed from small PS. The diameter of the polymer spheres of 179 nm, which was roughly estimated from the SEM images, was highly consistent with the value (178 nm) from DLS. With the progressive decrease of the T_g of the spheres from 112°C to −34°C, the curved surface surrounded by small PS became uniformly flat [Figure 2(b)], and the array of small PS gradually became less distinct [Figures 2(c–f)] until a nearly smooth surface without any discernible small PS was apparent [Figure 2(f)]. These observations are indicative of coalescence, fusion, and formation of a continuous phase during the film-formation process as the T_g of the polymer spheres decreased. However, the values of the diameters derived from DLS were consistently larger than those calculated from SEM. This may be attributed to shrinkage of the soft polymer spheres due to capillary force during the film-formation process, or the arranged small PS covered a part of top surface of sphere, which resulted in the discordant diameter values. It is well known that the mobility of molecular chains is strongly dependent on the T_g of the polymer. Because the T_g of the spheres is higher than the assembly temperature of 50°C, the mobility of the spheres in the polymer chain was restricted, and the polymer displayed glassy behavior. Thus, the distinct spherical shape was observed. As the T_g of the spheres decreased to below the assembly temperature, the mobility of the polymer chain increased to give a flexible, rubberlike polymer. Therefore, the polymer spheres coalesced slightly and fused with each other for sphere T_g values of 8°C and −20°C, thus covering part of the small PS in the cavity and interstices [Figures 2(d,e)]. When the T_g of the spheres was decreased to −34°C, the highly flexible polymer chains of the spheres coalesced even further and fused, thus obscuring the array constructed by the small PS, resulting in a nearly smooth surface, even though the long-range ordered structures of small PS were still embedded under the smooth surface.

As mentioned above, the ordered array embedded in the PBG film was constructed by small PS. The content of small PS plays an important role in preventing coalescence of the polymer spheres and ensuring the formation of the periodic structure. Although difficult to observe for the T_g of −34°C (Figure 2), spheres were used to construct the PBG film. Thus, PBG films employing spheres with the higher T_g of 26°C are presented, and the surface morphologies of the PBG films with various small PS contents are shown in Figure 3. In the case of insufficient small PS content, a pure polymer film was similarly apparent with many surface caves, and it was difficult to observe any visible ordered structure [Figure 3(a)]. When the small PS content of the film exceeded 10 wt %, the films exhibited an ordered array of polymer spheres [Figure 3(b–e)] and the surface caves disappeared. The caves were due to channels formed by evaporating water. As sufficiently rigid PS was filled into the PBG film, the interstices between the rigid PS provide channels to assist evaporation of water out of the film, thus the surface caves disappeared. The variation of the surface morphologies implied that the architectural construction was changed as illustrated in Figure 4. In the case of the PBG film with a low content of small PS, the small PS was insufficient for construction of the barriers to prevent coalescence, and thus, the polymer spheres collapsed. When the appropriate content of small PS was present, the polymer spheres were precisely enclosed by barrier ribs constructed by small PS, giving rise to the ordered structures. However, as progressive increased the small PS content, the polymer spheres were encircled by more than one layer of small PS. Added small PS layers were arranged along with the curve surface on sphere top, resulting in small encircled diameter.

Optical Properties of PBG Films

To ensure that the photonic stop bands were present in the PBG films of different softness, and that the long-range ordered structure was indeed embedded in the films, the PBG films constructed by varying the T_g of the spheres (constant small PS content of 10 wt %) were further examined by acquisition of the reflection spectra shown in Figure 5. The evidently monochromatic films ranging from blue to green exhibited sharp reflected peaks at the respective positions, which were blue-shifted from 562 nm to 462 nm as the T_g of the sphere increased from −34°C to 26°C. The films constructed with spheres having a T_g higher than 26°C exhibited inferior film properties with obvious cracks and fragments. The decrease in the stop band could be explained based on Bragg's diffraction law:

$$\lambda_{max} = 2d_{111}\sqrt{n_{eff} - \sin^2\theta} \quad (1)$$

where d_{111} represents the distance between the crystalline [111] planes in relation to the sphere diameter D; $d = 0.8165$ D based on the fcc structure. The symbol n_{eff} represents the effective refractive index, and in this experiment, n_{eff} is expressed by the following equation:

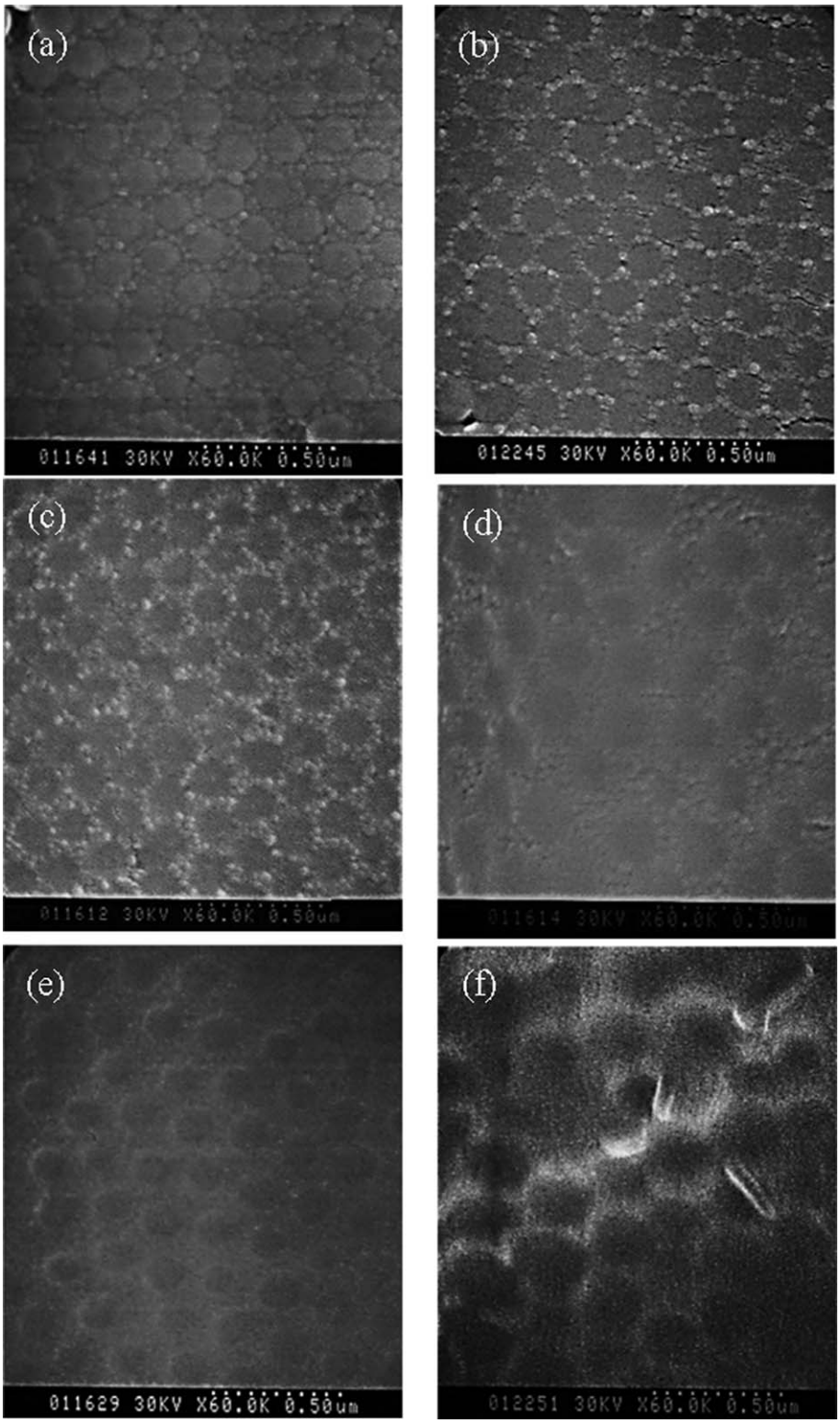

Figure 2. Surface morphologies of opal film constructed by various T_g spheres blended with 25 wt % small PS. (a) 112°C, (b) 50°C, (c) 26°C, (d) 8°C, (e) −20°C, (f) −34°C.

$$n_{\text{eff}} = \sqrt{f_{\text{polymer}} n^2{}_{\text{polymer}} + f_{(\text{PS+air})} n^2{}_{(\text{PS+air})}} \quad (2)$$

where f_{polymer} and $f_{(\text{PS + air})}$ are the filling ratio of the polymer spheres and of small PS plus air, respectively. Thus, the wavelength of the stop band not only increases in direct proportion to the diameter but is also affected by the refractive index of the spheres. As shown in Table I, the diameter of the spheres decreased dramatically from 281 nm to 153 nm as the T_g of the

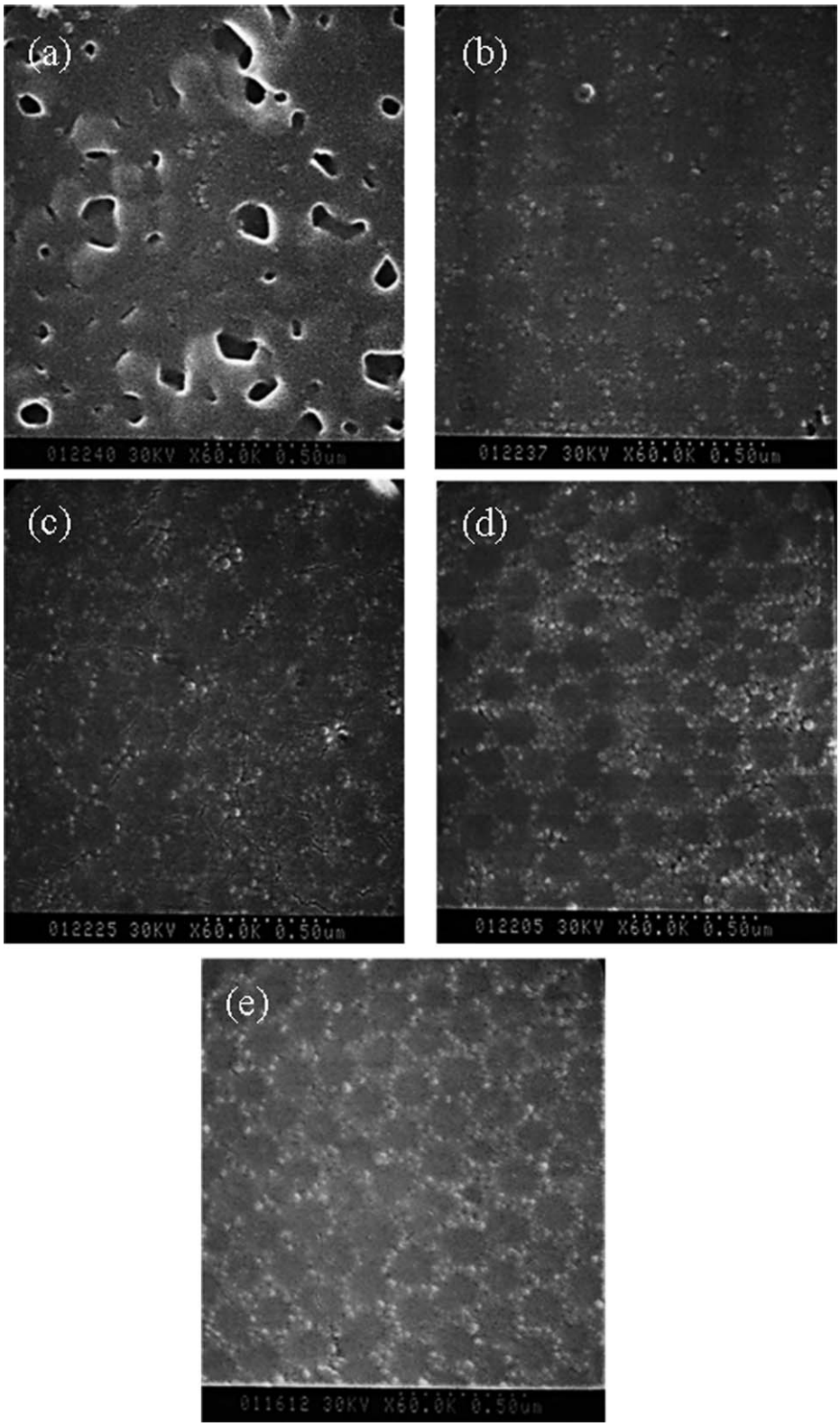

Figure 3. Surface morphologies of opal film prepared by 26°C T_g spheres blended with different small PS content. (a) 5 wt %, (b) 10 wt %, (c) 15 wt %, (d) 20 wt %, (e) 25 wt %.

spheres increased, with a consequent blue-shift of λ_{max}. Although calculation of the theoretical refractive index of the copolymer was difficult, the prediction of sphere diameter and n_{eff} were able to obtain by a straight line in the plot of λ_{max}^2 vs. $\sin^2\theta$ [from eq. (1)]. Therefore, the λ_{max} positions of PBG film constructed by T_g of −34°C spheres were recorded in different

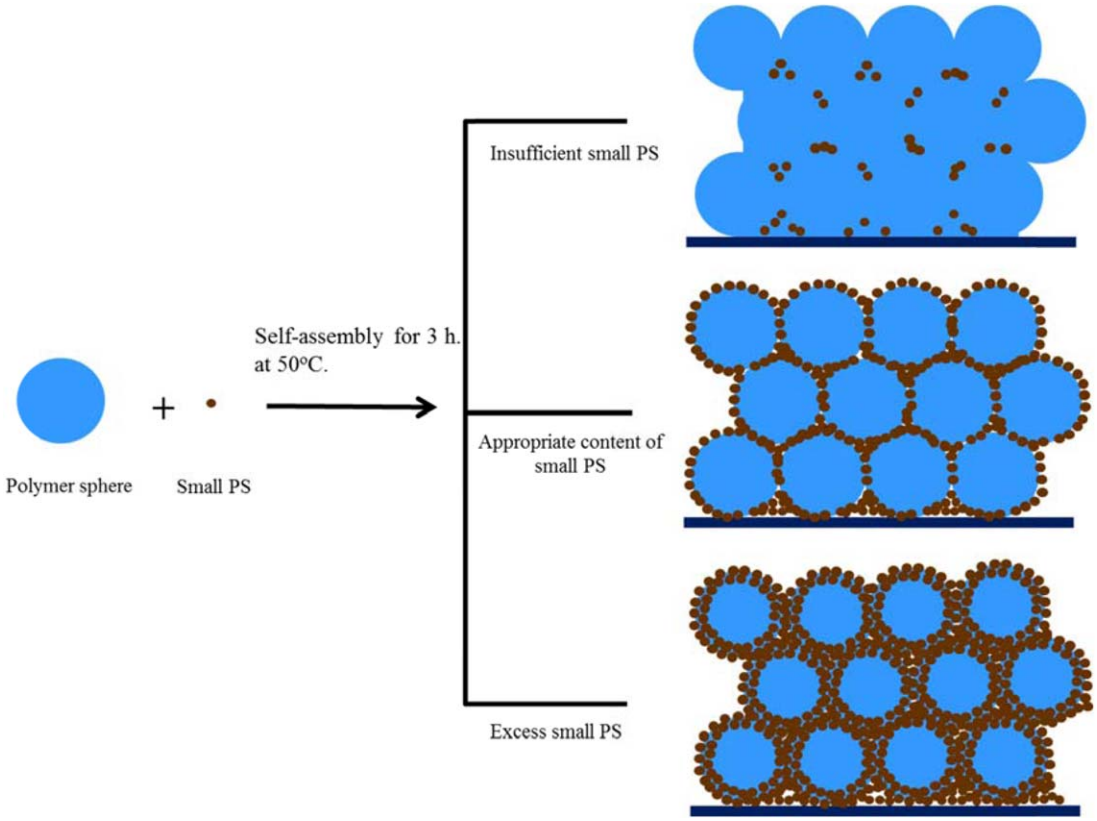

Figure 4. Illustrations of architectural construction prepared by different small PS content. [Color figure can be viewed in the online issue, which is available at wileyonlinelibrary.com.]

incident light directions, and the correlation plot shown in Figure 6. The very close results between fitted diameter (222 nm) and diameter from SEM (224 nm) confirmed that these structures exhibit Bragg diffraction, which also indicated that the fitted n_{eff} of PBG film was about 1.52. However, it also certified that the PBG film can be prepared by using spheres of various T_g.

Mechanical Properties of the PBG Film

Due to the generally inferior mechanical properties of colloid PBG films, many studies have focused on improving the film properties.[25–31] Herein, the PBG film was constructed from polymer spheres only. The mechanical properties could easily be controlled by two main approaches to satisfy the requirements of various specific applications. One strategy involves adjusting the T_g of the component polymer spheres, and the second involves varying the filling ratio of soft polymer spheres relative to small PS. These PBG films were subsequently subjected to tensile tests, recorded as stress–strain diagrams. The tensile

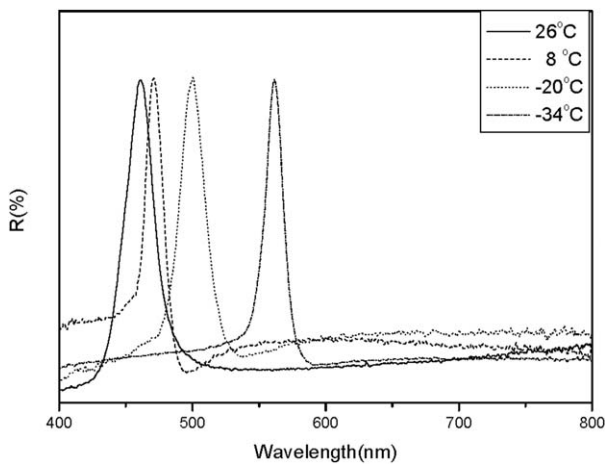

Figure 5. Reflection spectra of opal film Prepared from different T_g of polymer spheres blended with 10 wt % small PS.

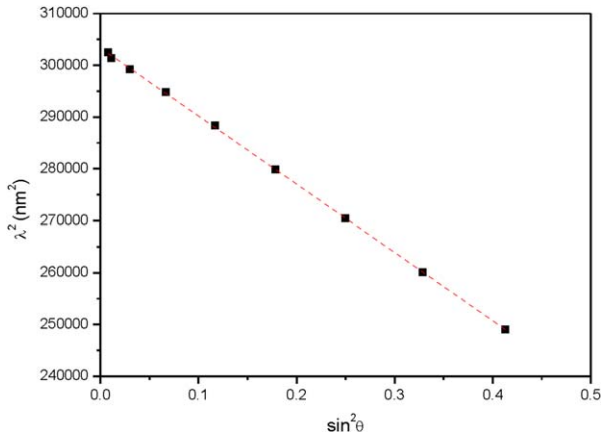

Figure 6. Plot of square of λ^2_{max} (reflection maxima) vs $\sin^2\theta$ of angle of incidence to the PBG film constructed by of −34°C spheres. [Color figure can be viewed in the online issue, which is available at wileyonlinelibrary.com.]

behavior of the PBG films constructed from spheres with various T_g using 10 wt % small PS is shown in Figure 7. A dramatic increase in the Young's modulus of the PBG films was observed as the T_g of the spheres increased from −34°C to 8°C, accompanied by an increase in the ultimate tensile strength from 0.65 Mpa to 4.7 Mpa, whereas the elongation declined from 828% to 16%. With progressive increase of the T_g of the spheres to exceed 26°C, the films exhibited cracks and even displayed powder-like properties, making it difficult to perform the tensile test. On the other hand, the characteristics of the stress–strain curves also gradually changed from typical elastomer type behavior to brittle plastic polymer behavior as the T_g of the spheres increased. A similar colloid PBG film constructed using core–shell spheres has been published by Hellmann's group, where the novel film-formation process of thermal uniaxial compression was necessary, during which, the hard cores were arranged into a crystalline lattice, and the soft shell was merged during flow in the melt. Although shear force and thermal extrusion were used to enhance the film properties, the ultimate tensile strength was still in the range of ca. 2.5 Mpa. Wu's group also successfully prepared organic/inorganic PBG films from blended spheres without the use of complex procedures. Soft spheres with T_g values of −2°C and 21°C were blended with small SiO_2, and subsequent drying at room temperature for 1 day furnished the elastic PBG film. The results of tensile tests indicated that the ultimate tensile strengths achieved were about 0.5 Mpa and 3 Mpa, respectively. Based on the aforementioned reports, the maximum recorded ultimate tensile strength of this type of colloid PBG films was about 3 Mpa, whereas the as-prepared organic/organic blend film developed herein exhibited a higher ultimate tensile strength of 4.7 Mpa.

To further extend the tunability of the PBG film, the spheres with a T_g of −34°C were blended with various amounts of small PS as a second approach; the tensile behaviors of the films are shown in Figure 8. Excellent deformability was achieved using 5 wt % small PS, with a film strain of 1236%. As the content of small PS in the film increased, the deformability exhibited a declining trend, accompanied by an increase in the ultimate tensile strength. The ultimate tensile strength reached 1.2 Mpa for a small PS content of 20 wt %, and the leathery property was

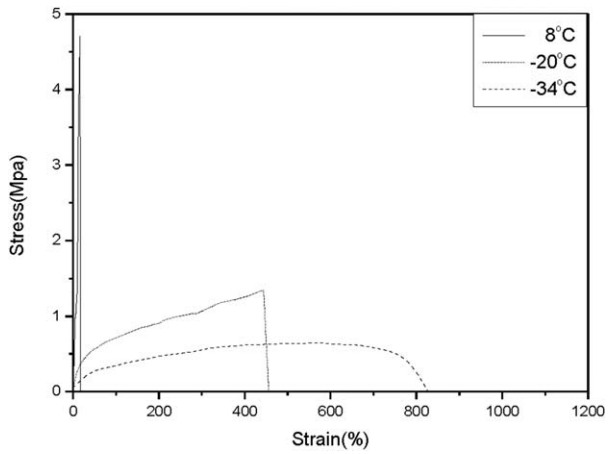

Figure 7. Stress–strain curves of opal film composed of different T_g of spheres and 10 wt % small PS.

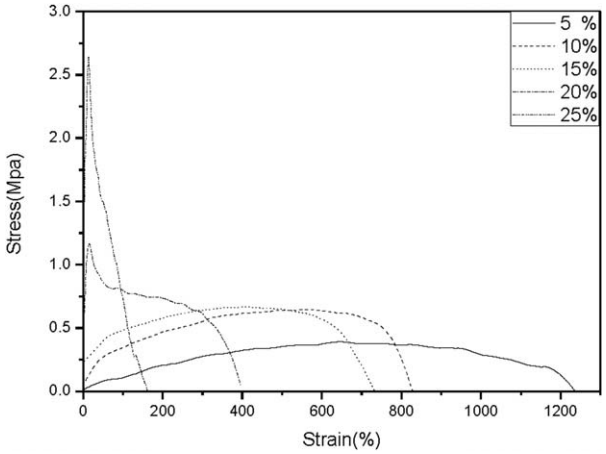

Figure 8. Stress–strain curves of opal film prepared by −34°C T_g spheres blended with different small PS content.

retained. However, the stress–strain curves deviated from typical elastomer behavior to brittle plastic polymer type behavior as the PS content was increased to 25 wt %. These results demonstrated that the mechanical properties of PBG films can be tuned by varying the small PS content in the range of 5–25 wt %.

CONCLUSION

In this study, a rapid, novel, and feasible approach for fabricating the PBG film was developed by blending two types of organic suspended spheres. Both types of spheres were synthesized by soap-free emulsion polymerization in the boiling state for 2 h. Spheres with a larger diameter (approximate D_n of 200 nm) and T_g values in the region between −45°C to 116°C were designed based on the Fox equation; the predicted T_gs of which were highly consistent with the T_g values from DSC. Small PS was synthesized with the aid of NaSS comonomer to ensure that the diameter was less than 50 nm. Blended suspensions of various compositions were subsequently self-assembled at 50°C for 3 h to obtain the PBG films. Evaluation of the architectural construction using SEM indicated that the soft polymer spheres were hexagonally arranged, and the small PS occupied the interstices when the appropriate PS filling ratio was utilized. Sharp PBG peaks observed in the UV–Vis spectra further confirmed that the PBG films could be constructed using spheres of various T_g. Variation of the diameter of the spheres from 281 nm to 153 nm effected a blue-shift of the maximum absorption of the tunable PBGs from 562 nm to 462 nm. Tensile tests indicated that the mechanical behavior of the PBG films can be tuned from typical elastomer behavior to brittle plastic polymer behavior with variation of the T_g of the component spheres from −34°C to 8°C, or by varying the PS filling ratio from 5 wt % to 25 wt %. Based on these two approaches, an ultimate tensile strength and a maximum elongation of 4.7 Mpa and 1236%, respectively, could be achieved.

REFERENCES

1. Yablonovitch, E. *Phys. Rev. Lett.* **1987**, *58*, 2059.
2. John, S. *Phys. Rev. Lett.* **1987**, *58*, 2486.

3. Mendioroz, L.; Gonzalo, R.; del Rio, C. *Microwave Optical Technol Lett.* **2001**, *30*, 81.
4. Kim, S.; Park, I.; Lim, H.; Kee, C. S. *Opt. Exp.* **2004**, *12*, 5518.
5. Zhu, C.; Chen, L. S.; Xu, H.; Gu, Z. Z. *Macromol. Rapid Commun.* **2009**, *30*, 1945.
6. Xie. Z. Y.; Sun, L. G.; Han, G. Z.; Gu, Z. Z. *Adv. Mater.* **2008**, *20*, 3601.
7. Kumoda, M.; Watanabe, M.; Takeoka, Y. *Langmuir* **2006**, *22*, 4403.
8. Xu, L. A.; Li, H.; Jiang, X.; Wang, J. X.; Li, L.; Song, Y. L.; Jiang, L. *Macromol. Rapid Commun.* **2010**, *31*, 1422.
9. Norton, J. C. S.; Han, M. G.; Jiang, P.; Shim, G. H.; Ying, Y. R.; Creager, S.; Foulger, S. H. *Chem. Mater.* **2006**, *18*, 4570.
10. Matsubara, K.; Watanabe, M.; Takeoka, Y. *Angew. Chem. Int. Ed.* **2007**, *46*, 1688.
11. O'Brien, P. G.; Puzzo, D. P.; Chutinan, A.; Bonifacio, L. D.; Ozin, G. A.; Kherani, N. P. *Adv. Mater.* **2010**, *22*, 611.
12. Ge, J. P.; Yin, Y. D. *Angew. Chem. Int. Ed.* **2011**, *50*, 1492.
13. Krauss, T. F.; DeLaRue, R. M.; Brand, S. *Nature* **1996**, *383*, 699.
14. Painter, O.; Lee, R. K.; Scherer, A.; Yariv, A.; O'Brien, J. D.; Dapkus, P. D.; Kim, I. *Science* **1999**, *284*, 1819.
15. Noda, S.; Chutinan, A.; Imada, M. *Nature* **2000**, *407*, 608.
16. Benisty, H.; Weisbuch, C.; Labilloy, D.; Rattier, M.; Smith, C. J. M.; Krauss, T. F.; De la Rue, R. M.; Houdre, R.; Oesterle, U.; Jouanin, C.; Cassagne, D. *J. Lightwave Technol.* **1999**, *17*, 2063.
17. Fink, Y.; Urbas, A. M.; Bawendi, M. G.; Joannopoulos, J. D.; Thomas, E. L. *J. Lightwave Technol.* **1999**, *17*, 1963.
18. Urbas, A.; Fink, Y.; Thomas, E. L. *Macromolecules* **1999**, *32*, 4748.
19. Kuo, Y. C.; Lee, Y. C.; Chen, H. *J. Thermoplast. Compos. Mater.* **2012**.
20. Xia, Y. N.; Gates, B.; Yin, Y. D.; Lu, Y. *Adv. Mater.* **2000**, *12*, 693.
21. Matijevic, E. *Langmuir.* **1994**, *10*, 8.
22. Zhang, S.; Zhao, X. W.; Xu, H.; Zhu, R.; Gu, Z. Z. *J. Colloid Interface Sci.* **2007**, *316*, 168.
23. Gu, Z.-Z.; Chen, H.; Zhang. S.; Sun, L.; Xie, Z.; Ge, Y. *Colloid Surf. A: Physicochem. Eng. Aspect.* **2007**, *302*, 312.
24. Fang, M.; Volotinen, T. T.; Kulkarni, S. K.; Belova, L.; Rao, K. V. *J. Nanophoton.* **2011**, 5.
25. McGrath, J. G.; Bock, R. D.; Cathcart, J. M.; Lyon, L. A. *Chem. Mater.* **2007**, *19*, 1584.
26. Lange, B.; Metz, N.; Tahir, M. N.; Fleischhaker, F.; Theato, P.; Schroder, H. C.; Muller, W. E. G.; Tremel, W.; Zentel, R. *Macromol. Rapid Commun.* **2007**, *28*, 1987.
27. Wohlleben, W.; Bartels, F. W.; Altmann, S.; Leyrer, R. J. *Langmuir.* **2007**, *23*, 2961.
28. Chen, X.; Wang, L. H.; Wen, Y. Q.; Zhang, Y. Q.; Wang, J. X.; Song, Y. L.; Jiang, L.; Zhu, D. B. *J. Mater. Chem.* **2008**, *18*, 2262.
29. Shen, Z. H.; Zhu, Y.; Wu, L. M.; You, B.; Zi, J. *Langmuir* **2010**, *26*, 6604.
30. Wohlleben, W.; Bartels, F. W.; Boyle, M.; Leyrer, R. J. *Langmuir* **2008**, *24*, 5627.
31. Tian, E. T.; Cui, L. Y.; Wang, J. X.; Song, Y. L.; Jiang, L. *Macromol. Rapid Commun.* **2009**, *30*, 509.
32. Gates, B.; Park, S. H.; Xia, Y. N. *Adv. Mater.* **2000**, *12*, 653.
33. Mayoral, R.; Requena, J.; Moya, J. S.; Lopez, C.; Cintas, A.; Miguez, H.; Meseguer, F.; Vazquez, L.; Holgado, M.; Blanco, A. *Adv. Mater.* **1997**, *9*, 257.
34. Miguez, H.; Tetreault, N.; Hatton, B.; Yang, S. M.; Perovic, D.; Ozin, G. A. *Chem. Commun.* **2002**, *2736*.
35. Wang, J. X.; Wen, Y. Q.; Ge, H. L.; Sun, Z. W.; Zheng, Y. M.; Song, Y. L.; Jiang, L. *Macromol. Chem. Phys.* **2006**, *207*, 596.
36. Fudouzi, H.; Sawada, T. *Langmuir* **2006**, *22*, 1365.
37. Ying, Y. R.; Foulger, S. H. *Sens. Actuat. B-Chem.* **2009**, *137*, 574.
38. Ying, Y. R.; Xia, J. Q.; Foulger, S. H. *Appl. Phys. Lett.* **2007**, 90.
39. Foulger, S. H.; Jiang, P.; Lattam, A.; Smith, D. W.; Ballato, J.; Dausch, D. E.; Grego, S.; Stoner, B. R. *Adv. Mater.* **2003**, *15*, 685.
40. Zhao, Q. B.; Haines, A.; Snoswell, D.; Keplinger, C.; Kaltseis, R.; Bauer, S.; Graz, I.; Denk, R.; Spahn, P.; Hellmann, G.; Baumberg, J. J. *Appl. Phys. Lett.* **2012**, *100*.
41. Imai, Y.; Finlayson, C. E.; Goldberg-Oppenheimer, P.; Zhao, Q. B.; Spahn, P.; Snoswell, D. R. E.; Haines, A. I.; Hellmann, G. P.; Baumberg, J. J. *Soft Matter.* **2012**, *8*, 6280.
42. Finlayson, C. E.; Haines, A. I.; Snoswell, D. R. E.; Kontogeorgos, A.; Vignolini, S.; Baumberg, J. J.; Spahn, P.; Hellmann, G. P. *Appl. Phys. Lett.* **2011**, *99*.
43. Finlayson, C. E.; Goddard, C.; Papachristodoulou, E.; Snoswell, D. R. E.; Kontogeorgos, A.; Spahn, P.; Hellmann, G. P.; Hess, O.; Baumberg, J. J. *Opt. Exp.* **2011**, *19*, 3144.
44. Snoswell, D. R. E.; Kontogeorgos, A.; Baumberg, J. J.; Lord, T. D.; Mackley, M. R.; Spahn, P.; Hellmann, G. P. *Phys. Rev. E.* **2010**, *81*.
45. Kontogeorgos, A.; Snoswell, D. R. E.; Finlayson, C. E.; Baumberg, J. J.; Spahn, P.; Hellmann, G. P. *Phys. Rev. Lett.* **2010**, *105*.
46. Viel, B.; Ruhl, T.; Hellmann, G. P. *Chem. Mater.* **2007**, *19*, 5673.
47. Ahles, M.; Ruhl, T.; Hellmann, G. P.; Winkler, H.; Schmechel, R.; von Seggern, H. *Opt. Commun.* **2005**, *246*, 1.
48. Ruhl, T.; Spahn, P.; Winkler, H.; Hellmann, G. P. *Macromol. Chem. Phys.* **2004**, *205*, 1385.
49. Ruhl, T.; Spahn, P.; Hellmann, G. P. *Polymer* **2003**, *44*, 7625.
50. Ruhl, T.; Hellmann, G. P. *Macromol. Chem. Phys.* **2001**, *202*, 3502.
51. Shen, Z. H.; Shi, L.; You, B.; Wu, L. M.; Zhao, D. Y. *J. Mater. Chem.* **2012**, *22*, 8069.
52. Duan, LL.; You, B.; Wu, L. M.; Chen, M. *J. Colloid Interface Sci.* **2011**, *353*, 163.
53. You, B.; Wen, N. G.; Shi, L.; Wu, L. M.; Zi, J. *J. Mater. Chem.* **2009**, *19*, 3594.
54. Liu, Y. Y.; Lin, H. M.; Chan, H. *Mol. Cryst. Liquid Cryst.* **2011**, *534*, 124.
55. Liu, Y. Y.; Lo, M. Y.; Chen, H. *J. Appl. Polym. Sci.* **2011**, *120*, 2945.